80-micron interaction length silicon photonic crystal waveguide modulator

Yongqiang Jiang[1, a)], Wei Jiang[1,2, a)], Lanlan Gu[1], Xiaonan Chen[1], Ray T. Chen[1, b)]
[1]*Microelectronic Research Center, Department of Electrical and Computer Engineering, The University of Texas at Austin, Austin, TX 78758, USA*
[2]*Omega Optics, Austin, TX 78758, USA*

(Received 25 July 2005; accepted 21 September 2005; published online 28 November 2005)

An ultra-compact silicon electro-optic modulator was experimentally demonstrated based on silicon photonic crystal (PhC) waveguides for the first time to our knowledge. Modulation operation was demonstrated by carrier injection into an 80 μm-long silicon PhC waveguide of a Mach-Zehnder interferometer (MZI) structure. The π phase shift driving current, I_π, across the active region is as low as 0.15 mA, which is equivalent to a V_π of 7.5 mV when a 50 Ω impedance-matched structure is applied. The modulation depth is 92%. © *2005 American Institute of Physics.*
[DOI: 10.1063/1.2077836]

Photonic crystals (PhCs) are a class of artificial optical materials with periodic dielectric structures, which result in unusual optical properties. PhCs now show promise to be a key platform for future optical integrated circuits [1-3]. Due to the unique properties of PhCs, the size of many optical components is anticipated to be greatly reduced by employing PhC structures, such as photonic crystal waveguides. In the most commonly employed configuration, a photonic crystal waveguide is formed by introducing a line defect into a two-dimensional (2D) PhC slab [4-15]. In such PhC waveguides, light is confined by a combination of in-plane PBG confinement and vertical index guiding. A size reduction mechanism based on slow group velocity in photonic crystal waveguides has been discussed for an array of optical devices [15]. Notomi *et al.* firstly demonstrated low group velocity and high group velocity dispersion using silicon PhC slab line defect waveguides [8]. Several other groups also demonstrated this effect in both line-defect and coupled-cavity PhC waveguides [12-15].

In the context of microelectronics, silicon has been the optimal material for microelectronics for a long time, but it has only relatively recently been considered as an option for photonics [16-18]. Silicon is transparent in the range of optical telecommunication wavelengths, 1.3 μm and 1.55 μm, and has high refractive index that allows for the fabrication of high-index-contrast nano-photonic structures. In addition, as silicon photonics technology is compatible with conventional complementary metal-oxide-semiconductor (CMOS) processing, monolithic integration of silicon photonic devices with advanced electronics on a single silicon substrate becomes possible. Optical modulators are pivotal components in silicon based optoelectronic integrated circuits. Most silicon electro-optic modulators are based on plasma dispersion effect, through which carrier concentration perturbation results in refractive index change [16-18]. There are a number of ways to vary the carrier concentration in silicon including carrier injection and capacitive coupling though the metal-oxide-semiconductor (MOS) field effect [19-22]. For broadband optical intensity modulators, the silicon Mach-Zehnder Interferometer (MZI) structure that converts a phase modulation into an intensity modulation is widely used [19-22]. However, conventional silicon MZI modulators are based on rib waveguides, which usually need one-half to several millimeters to achieve the required phase shift in MZI structures [19-22]. The reason is that propagation constant perturbation, $\Delta\beta$, is fairly low, thus requiring larger rib waveguide length, L, to achieve required phase shift, $\Delta\phi = \Delta\beta \times L$.

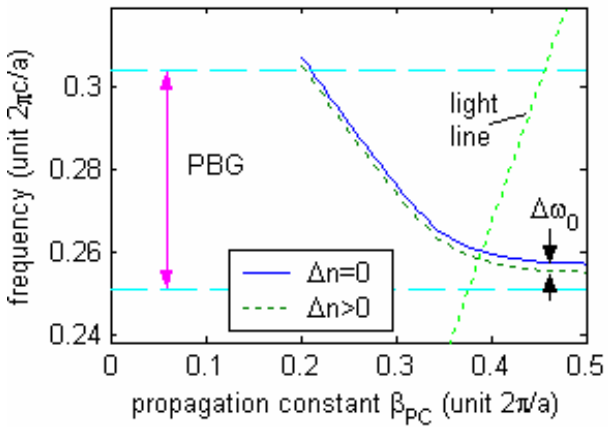

FIG. 1. Dispersion relation of a guide mode of a photonic crystal waveguide

The extraordinary dispersion of photonic crystal (PhC) waveguides offers an unprecedented opportunity for developing ultra-compact MZI modulators. Consider a typical dispersion relation for a PhC waveguide mode shown in Fig. 1. If the refractive index of the waveguide core material (*i.e.* silicon) varies by an amount of Δn, the dispersion curve will shift vertically by an amount $\Delta\omega_o$. As theoretically explained by Soljacic et al.[15], for a fixed frequency of light, the propagation constant β_{PC} of PhC waveguide changes as

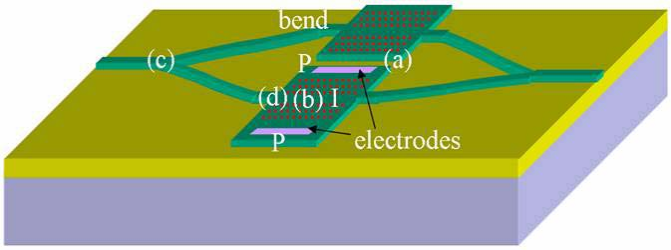

FIG. 2. Schematic diagram of the silicon Mach-Zehnder PhC modulator. Electrode structure of the modulator with PIP regions indicated.

$\Delta\beta_{PC} = \frac{d\beta_{PC}}{d\omega}\Delta\omega_0$, which grows significantly whenever the group velocity $\frac{d\omega}{d\beta_{PC}}$ approaches zero, e.g. on the right-most segment of dispersion curve in Fig. 1. Such an extraordinary growth of $\Delta\beta_{PC}$ directly leads to a significant enhancement of phase modulation efficiency because the phase change is related to the change of propagation constant and waveguide length L as $\Delta\phi_{PC} = \Delta\beta_{PC} \times L$. One can easily enhance $\Delta\beta_{PC}$ by more than 100 times using a photonic crystal waveguide. Therefore, a 100 times shorter PhC waveguide can produce the same phase change as a long conventional waveguide.

The short device length is a benign feature for many other device performance considerations. The optical modulator device has a short PhC waveguide of a few tens of microns in length, which promises a low propagation loss. The power dissipation of the modulator is also expected to be one to two orders of magnitude lower owing to the much shorter electrode length.

A schematic of a silicon MZI modulator is shown in Fig. 2. The MZI modulator is composed of PhC waveguides, rib waveguides, Y-junctions, electrodes, and electrode pads. PhC waveguides are used in both arms of the MZI modulator to ensure the two arms have the same optical loss and dispersion; otherwise the modulation depth may suffer a reduction.

PhC waveguides of the MZI modulator are designed, fabricated and characterized [23]. A line-defect (W-1) PhC waveguide can be easily generated by removing a single row of air holes from a 2-D PhC slab. The dispersion diagram of PhC waveguides is calculated using the 3-D fully vectorial plane-wave expansion (PWE) method [24]. The slab is fabricated on a silicon-on-insulator (SOI) wafer. The thickness of the silicon core layer is t = 215 *nm*. The top cladding is air and the bottom cladding is a buried oxide layer of 2 μm thick. The pitch size of the hexagonal PhC lattice is a = 400 *nm*. The normalized air hole diameter is designed to be d/a = 0.53.

To fabricate the ultra-compact silicon MZI modulator, the designed PhC waveguides, rib waveguides, and Y-junctions are first fabricated on a SOI wafer. A PIP structure is formed by an implantation of boron at 25 keV with a peak concentration of 2×10^{17} cm^{-3} into an N-type Si substrate with the doping concentration of 1×10^{14} cm^{-3}. Medici simulation tool shows the P-I-P diode injects holes only. The PIP I-V curve is experimentally confirmed for both forward and reverse biases. Note that the N-type Si substrate with 1×10^{14} cm^{-3} doping concentration is defined as intrinsic [25]. The PhC and Si rib waveguide structures are patterned with E-beam resist ZEP-520A by E-beam lithography (Jeol JBX6000). After developing the resist, the patterns are transferred to a 57 nm oxide mask layer by reactive ion etching (RIE) using CHF_3. Then the E-beam resist residue is removed by plasma ashing in oxygen. Using the oxide layer as a hard mask the patterns are transferred to the silicon core layer by a HBr and Cl_2 RIE process. Post-etching oxidation at 850°C is implemented for about 1 minute. The post-etching oxidation forms an additional 5~7nm oxide layer, resulting in the sidewalls of the air-holes being significantly smoother than the original surface after dry etching [23]. Extensive experimentation with various processes is conducted to determine the optimized process parameters. A proper pre-offset of the hole size in e-beam pattern design is used so that the hole size can be controlled with an accuracy of 5%. After the silicon photonic crystal waveguides and rib waveguides are fabricated, the regions for the aluminum electrodes and pads are patterned by a conventional photolithography mask aligner, followed by metal deposition and metal liftoff. Aluminum electrodes and pads are then sintered to form ohmic contacts with the top silicon layer. The SEM picture of the final structure is shown in Fig. 3, with the corresponding sections marked in Fig. 2.

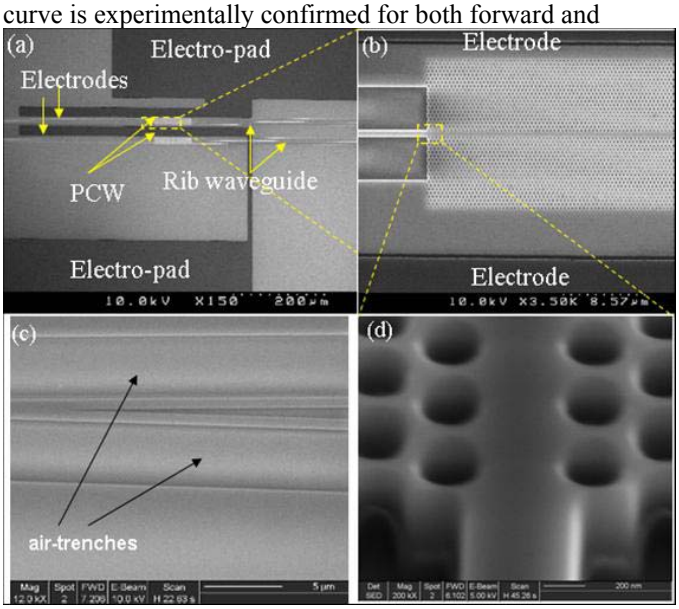

FIG. 3. SEM pictures of the silicon PhC modulator: (a) overview picture of the modulator. (b) PhC waveguide with two electrodes. (c) Y-junction. (d) Magnified PhC waveguide based on a triangular lattice with lattice constant a=400nm, hole diameter d = 210 nm, and top Si thickness t = 215 nm, buried oxide (BOX) SiO_2 thickness of 2 μm.

For the optical measurement, we introduce a silicon rib waveguide bend [26], which shifts the output silicon rib waveguide by at least 600 μm and significantly suppresses the stray light collected by the output fiber. The measurement is performed on a fully-automated Newport Photonics

Alignment/Packaging Station. Two lensed fibers are manipulated by two automated 5-axis stages, which are controlled by a computer to precisely align the fibers with the rib waveguides. The input lensed fiber is aligned for the transverse electrical (TE) mode with the electric field vector primarily in plane. The TE polarized light is used for all the measurement presented here. The propagation loss of passive photonic crystal waveguides fabricated with the aforementioned processing sequence is around 6 dB/mm [23]. Note that the waveguides fabricated without post-etching oxidation typically have propagation loss over 20 dB/mm, which manifests the advantage of oxidation.

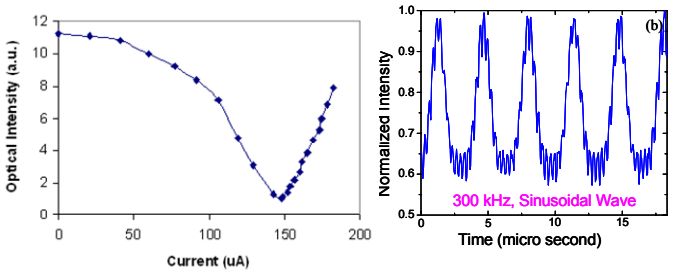

FIG. 4. Modulation characteristics (a) Intensity vs. injection current, 92% modulation depth is achieved at 0.15mA; (b) Modulation curve of 300 kHz sinusoidal wave with peak current of 0.11 mA.

We investigate the modulation performance of the fabricated modulators. We characterize the modulation depth and the minimum current needed for phase shift of π, I_π, of our silicon MZI modulator operating at 1567 nm. We have measured the transmission spectra which confirm that 1567 nm falls into the bandedge of the transmission spectra. The optical output intensity against drive current is shown in Fig. 4(a). The modulation depth of 92% is clearly seen in Fig. 4(a). The modulated signal is displayed in Fig. 4(b) with sinusoidal input signal at 300 kHz. The π radian drive current, I_π, is a typical measure of the quality of such MZI modulator devices. The I_π of our silicon MZI modulator is as low as 0.15 mA compared to several mA in conventional MZI modulator devices [17-18], which shows the high quality of our MZI modulator device. With a 50 Ω impendence matched lumped electrode structure, it is equivalent to a V_π of 7.5 mV. The length of the modulator is reduced to 80 μm compared to several millimeters for the modulators using silicon rib waveguides in MZI structures [15-16], due to the extraordinary dispersion of the PhC waveguide. All of these prove the proposed advantages of using PhC waveguide instead of conventional rib waveguide mentioned above. The thermo-optic effect is excluded as a mechanism for phase shift, because the power dissipation I^2R is very low, and the subsequent temperature rise of the waveguide only less than 0.3 ^oC.

In conclusion, we designed, fabricated, and characterized an ultra-compact silicon electro-optic modulator based on silicon photonic crystal waveguides with a hexagonal lattice of air holes. Modulation operation was demonstrated by carrier injection into an 80 μm-long silicon photonic crystal waveguide. The modulation depth is over 92%. The I_π is as low as 0.15 mA. Further improvement in device performance is expected by optimizing the electrode design and reducing the contact resistance.

This research is supported in part by AFOSR. Technical advice from Drs. Gernot Pomrenke and Richard Soref is acknowledged. The authors are indebted to the State of Texas and SEMATECH for support under the AMRC program. The devices were fabricated at UT MRC with nanofabrication facilities partially supported under NSF's NNIN program. We thank the CNM of UT Austin, Welch Foundation and SPRING for partial support of the Dual Beam FIB/SEM usage. We appreciate Dr. J. R. Cao of the University of Southern California and Dr. B.L. Miao of the University of Delaware for fruitful discussions.

[a] Yongqiang Jiang and Wei Jiang have equal contribution to this work.
[b] Author to whom correspondence should be addressed; Email: chen@ece.utexas.edu

[1]E. Yablonovitch, Phys. Rev. Lett. **58**, 2059 (1987)
[2]S. John, Phys. Rev. Lett. **58**, 2486 (1987)
[3]J.D. Joannopoulos, R.D. Meade, J.N. Winn, Photonic Crystals, Princeton University Press (1995)
[4]S.G. Johnson et al, Phys. Rev. B **60**, 5751 (1999)
[5]M. Tokushima, et al, App. Phys. Lett. **76**, 952 (2000)
[6]M. Loncar et al, Appl. Phys. Lett. **77**, 1937 (2000)
[7]S. J. McNab et al, Opt. Express **11**, 2927 (2003)
[8]M. Notomi et al, Phys. Rev. Lett. **87**, 253902 (2001)
[9]T. Baba et al, J. Selected Topics Quan. Electr. **10**, 484 (2004)
[10]W. Bogaerts, et al, J. Lightwave Technology 23, 401 (2005)
[11]B.L. Miao, et al, IEEE Photo. Tech. Lett. **16**, 2469 (2004)
[12]T. Asano, et al, App. Phys. Lett. **84**, 4690 (2004)
[13]D. Mori, T. Baba, App. Phys. Lett. **85**, 1101 (2004)
[14]T.J. Karle, et al, J. Lightwave Technology 22, 514 (2004)
[15]M. Soljacic, J.D. Joannopoulos, Nature materials 3, 211 (2004); M Soljacic, S. G. Johnson, S. Fan, M. Ibanescu, E. Ippen, J. D. Joannopoulos, J. Opt. Soc. Am. B 19, 2052 (2002)
[16]R. A. Soref, B. R. Bennett, IEEE J. Quantum Electron. QE-23, 123 (1987)
[17]R. A. Soref, Proc. SPIE, 5730, 19 (2005)
[18]G. Reed, A. P. Knights, Silicon Photonics, an introduction, John Wiley & Sons (2004)
[19]A. Liu, R. Jones, L. Liao, D. Samara-Rubio, D. Rubin, O. Cohen, R. Nicolaescu, and M. Paniccia., Nature 427, 615 (2004)
[20]L. Liao, D. Samara-Rubio, M. Morse, A. Liu, D. Hodge, D. Rubin, U. D. Keil, and T. Franck, Opt. Express 13, 3129 (2005)
[21]C.Z. Zhao, G.Z. Li, E.K. Liu, Y. Gao, and X.D. Liu, Appl. Phys. Lett. 67, 2448 (1995)
[22]G.V. Treyz, P.G. May and J.M. Halbout, Appl. Phys. Lett., 59, 771 (1991)
[23]Y. Q. Jiang, W. Jiang, X. N. Chen, L. L. Gu, B. Howley, R. T. Chen, Proc. SPIE 5733, 166 (2005)
[24]S. G. Johnson and J. D. Joannopoulos, Optics Express 8, 173 (2001)
[25]B. Streetman, S. Banerjee, Solid State Electronic Devices, Prentice Hall (1999)
[26]M. Zelsmann, et al, J. Appl. Phys. 95, 1606 (2004)

